

## Compensating Silicon calorimetry for the next generation of hadronic colliders

SICAPO Collaboration

E. Borchi <sup>1</sup>, C. Furetta <sup>2,a</sup>, P. Giubellino <sup>3</sup>,  
F. Lamarche <sup>4</sup>, C. Leroy <sup>4</sup>, R. Macii <sup>1</sup>,  
C. Manoukian-Bertrand <sup>4</sup>, R. Paludetto <sup>2</sup>, S. Pensotti <sup>2,b</sup>,  
A. Penzo <sup>5</sup>, L. Ramello <sup>3,c</sup>, P.G. Rancoita <sup>2</sup>,  
L. Riccati <sup>3</sup>, G. Salvato <sup>5,d</sup>, A. Seidman <sup>2,e</sup>,  
A. Villari <sup>5,f</sup> and L. Vismara <sup>2</sup>

<sup>1</sup> INFN-Florence and at University, Florence, Italy

<sup>2</sup> INFN-Milan, Milan, Italy

<sup>3</sup> INFN-Turin, Turin, Italy

<sup>4</sup> Université de Montréal, Montréal (Québec), Canada

<sup>5</sup> INFN-Trieste, Trieste, Italy

<sup>a</sup> and University of Rome, Rome, Italy

<sup>b</sup> and University of Milan, Milan, Italy

<sup>c</sup> and University of Turin, Turin, Italy

<sup>d</sup> and CNR of Messina, Messina, Italy

<sup>e</sup> and Tel-Aviv University, Tel-Aviv, Israel

<sup>f</sup> and University of Messina, Messina, Italy

### Abstract

The compensation condition ( $e/\pi = 1$ ) is discussed. It mainly determines the performances of the silicon calorimeters to be used at the next generation of hadronic colliders (LHC, SSC, UNK).

Presented at the 2nd Int. Conf. on Advanced Technology in Particle Physics,  
Villa Olmo, Como, Italy, June 1990.

To be published in Proceedings, to appear in Nuclear Physics B, Suppl.

## 1. Introduction

The search for heavy leptons, supersymmetric particles, the Higgs particle(s), and the additional vector bosons predicted in many possible extensions of the Standard Model is part of a vast research programme to be carried out by the future experiments at the next generation of colliders [the Large Hadron Collider (LHC) in the LEP tunnel at CERN, the Superconducting Super Collider (SSC) in the USA, and the Accelerating and Storage Complex (UNK) in the USSR].

The possibility of achieving these research programmes will rely on highly performant detection systems. High luminosities and high multiplicities in a high-level radiation environment will characterize the operation of these colliders and challenge the performances of the hadron calorimeter constituting the core element of the central detection system.

The physics goals, and the processes that limit the effective energy resolution, fix the required calorimeter energy resolution at  $\sim 50\%/\sqrt{E}$  [1]. The conditions to be satisfied in order to obtain that energy resolution with a silicon hadron calorimeter are given in the present paper.

## 2. $e/mip$ , $h/mip$ and $e/\pi$ ratios

### 2.1 The $e/mip$ ratio

The electromagnetic processes at work during cascading have large cross-sections, and nuclear interactions play no role in the energy deposition. Therefore the electromagnetic cascading depends essentially on the density of electrons in the absorber medium and is precisely described [2] by Quantum Electrodynamics (QED). As a consequence, the behaviour of the electromagnetic showers in a calorimeter is well understood and so is the response of calorimeters to electromagnetic cascading. In the process of energy deposition, the incident energy is shared among the large number of secondary particles created by bremsstrahlung and electron-pair production. These two processes become practically energy independent beyond 1 GeV. The mean path-length of an electron in a material ( $A, Z$ ) is given approximately by [3]:

$$X_0 \approx 180 (A/Z^2) [\text{g/cm}^2], \quad (1)$$

where  $X_0$  is the radiation length and characterizes the longitudinal development of the shower.

Beyond its maximum, the shower decays slowly via ionization and Compton scattering. The multiple Coulomb scattering of the electrons is the main contribution to the radial spread of the shower: these electrons have an energy sufficient to travel away from the shower axis. The natural transverse unit of a shower is the Molière radius  $R_M$  and is defined as the lateral spread of an electron beam of energy  $\epsilon$  after traversing a thickness  $X_0$ :

$$R_M = (E_M/\epsilon)X_0,$$

where  $E_M = 21$  MeV and  $\epsilon$  is the critical energy. The latter is the energy of an electron that loses as much energy in collisions as in radiation and can be expressed as [4]:

$$\epsilon = B(ZX_0/A)^a [\text{MeV}] \quad (2)$$

with the radiation length  $X_0$  in  $\text{g/cm}^2$  as given by expression (1),  $A$  is the atomic mass,  $B = 2.66$ , and  $a = 1.11$ . For a rapid estimate of the Molière radius, one can also use the

expression [3]:

$$R_M \approx 7 A/Z [\text{g/cm}^2].$$

The 95% radial containment ( $R_e$ ) and the 95% longitudinal containment ( $L_e$ ) for electromagnetic showers are respectively (in units of radiation length):

$$R_e(95\%) = 2 R_M$$

$$L_e(95\%) = (t_{\max} + 0.08Z + 9.6) [X_0],$$

where  $t_{\max} = 1.0(\ln E/c - l)$  ( $l = 1$  and  $0.5$  for electrons and photons respectively,  $E$  in GeV).

The ratio  $e/mip$  measures the energy deposited in the sensitive part of the calorimeter by electron and photon showers relative to the energy deposited by minimum ionizing particles. The energy shared ( $E_s$ ) by a minimum ionizing particle in the silicon detectors is given by

$$E_s = \frac{(dE/dx)_{Si} X_{Si} E}{[(dE/dx)_{Si} L_{Si} + \sum (dE/dx)_i L_i]}, \quad (3)$$

where,  $X_{Si}$ ,  $L_{Si}$ ,  $L_i$ ,  $(dE/dx)_i$ , and  $E$  are the depletion depth, the thickness of the Si detector, the thickness of the absorber  $i$ , the average energy loss per unit of length in the absorber  $i$ , and the incoming particle energy, respectively.

The  $e/mip$  ratio is therefore defined as

$$e/mip = \epsilon_{vis}(e)/E_s$$

where  $\epsilon_{vis}(e)$  is the visible electromagnetic energy measured in the calorimeter, and  $E_s$  is given by expression (3).

## 2.2 The $\pi/mip$ and $h/mip$ ratios

Analogously, a ratio  $\pi/mip$  can be defined and measures the energy deposited by hadrons relative to the energy deposited. The hadronic shower is propagated through a succession of various inelastic interactions leading to multiparticle production characterized by a multiplicity increasing logarithmically with the available energy ( $\approx \ln s$ ). From the primary energy, half is carried away by leading-particles and the second half absorbed in the production of secondaries, mainly pions and nucleons. The longitudinal development of a hadronic shower is described in units of the nuclear interaction length:

$$\lambda = A/(N_{av} \rho \sigma_i) [\text{cm}] \approx 35 A^{1/3} [\text{g/cm}^2], \quad (4)$$

where  $A$ ,  $N_{av}$ ,  $\rho$ , and  $\sigma_i$ , are the mass number, the Avogadro number, the density of the material, and the proton inelastic cross-section, respectively. The behaviour of  $\sigma_i$  with energy reflects the smooth dependence of hadron production on the energy and the type of projectile. Therefore  $\lambda$  is practically constant at energies well above the resonance region and is about equal for the primary and secondary particles and justifies its choice as the unit to describe the containment of a hadronic shower.

The 95% radial containment ( $R_\pi$ ) and the 95% longitudinal containment ( $L_\pi$ ) for hadronic showers are respectively [5] [in units of  $\lambda$ , cf. Eq. (4)]:

$$R_\pi(95\%) \leq 1 [\lambda] \quad (E \text{ in GeV})$$

$$L_{\pi}(95\%) \approx t_{\max} + 2.5\lambda_{\text{att}},$$

where

$$t_{\max} \approx 0.2 \ln E + 0.7 \quad (E \text{ in GeV})$$

is the shower maximum and depends on  $\lambda$ , and  $\lambda_{\text{att}}$  describes the exponential decay of the shower beyond  $t_{\max}$  and varies with energy as

$$\lambda = \lambda[E(\text{GeV})]^{0.13}.$$

The ratio  $\pi/\text{mip}$  is defined as:

$$\pi/\text{mip} = \epsilon_{\text{vis}}(\pi)/E_s,$$

where  $\epsilon_{\text{vis}}(\pi)$  is the visible hadronic energy measured in the calorimeter.

Normally, after the primary interaction, decays of hadronic resonances created during the degradation of the energy of the incident hadrons and charge-exchange reactions produce  $\pi^0$  (mainly) and  $\eta$ , which will propagate electromagnetically without any further nuclear interactions and consequently deposit their energy in the form of electromagnetic showers. As a result, any hadronic shower has a purely hadronic and a purely electromagnetic component. The size of this electromagnetic component is largely determined by the production of  $\pi^0$  (and  $\eta$ ) in the first interaction.

In the extreme case where there is no generation of an electromagnetic component in the hadronic shower, similarly to  $\pi/\text{mip}$ , one can define an  $h/\text{mip}$  ratio:

$$h/\text{mip} = \epsilon_{\text{vis}}(h)/E_s,$$

where  $\epsilon_{\text{vis}}(h)$  is the visible pure hadronic energy measured in the calorimeter in the absence of an electromagnetic component in the shower.

Therefore the total visible energy can now be expressed as:

$$\epsilon_{\text{vis}}(\pi) = E_s f_{\text{em}} (e/\text{mip}) + E_s (1 - f_{\text{em}}) (h/\text{mip}), \quad (5)$$

where  $f_{\text{em}}$  is the average fraction of the converted electromagnetic energy resulting from the decays of  $\pi^0$ 's,  $\eta$ 's and vector mesons produced during the hadron cascade. The average fraction converted into an electromagnetic shower increases with energy. For instance, the total number of  $\pi^0$  in a shower initiated by  $\pi^+$  (in Fe) slowly increases with energy as [3]:

$$n_{\pi^0} \approx 5 \ln E (\text{GeV}) - 4.6.$$

Since the electromagnetic fluctuations are partially compensated by the energy dissipated by relativistic charged particles and by fast protons,  $f_{\text{em}}$  is also expected to increase smoothly with the incident energy<sup>1)</sup>.

### 2.3 The $e/\pi$ ratio

The fact that only a small fraction of the energy is deposited in the active layers and contributes to the calorimeter signal is the origin of sampling fluctuations ( $\sigma_{\text{samp}}$ ). Since it is mainly generated by the fluctuation in the total number of charged particles crossing the active layers, the contribution of this source of fluctuations is proportional to the square root of the thickness of the absorber plates ( $t_{\text{abs}}$ ).

---

1)  $f_{\text{em}}(E) \approx 0.1 \ln E(\text{GeV})$  for  $10 < E < 100 \text{ GeV}$ .

A large amount of the deposited energy in a calorimeter goes in breaking nuclei (binding energy) or in low-energy neutrons and therefore is partially not visible. In addition, pion and muon decays produce secondary particles such as  $\nu$  which are undetected. The amount of energy converted into excitation, or break-up of the nuclei, fluctuates from event to event. These intrinsic fluctuations ( $\sigma_{\text{intr}}$ ) contribute to the energy resolution. Therefore, the energy resolution of the calorimeter can be generally written as:

$$\sigma/E = C(\sqrt{t_{\text{abs}}})/\sqrt{E} + \phi((e/\pi) - 1),$$

where  $C = (\sigma_{\text{intr}}^2 + \sigma_{\text{samp}}^2)^{1/2}$ .

The  $e/\pi$  signal ratio is defined as

$$e/\pi = \frac{(e/\text{mip})}{[(e/\text{mip})f_{\text{em}} + (h/\text{mip})(1 - f_{\text{em}})]}, \quad (6a)$$

which can be rewritten as

$$e/\pi = \frac{(e/h)}{[1 - f_{\text{em}}(1 - e/h)]}. \quad (6b)$$

Equation (6b) shows that  $e/h = 1$  obviously implies  $e/\pi = 1$  and vice versa.

The nuclear effects, which dominate pure hadronic showers, have no counterpart in electromagnetic showers. Therefore, the calorimeter response to the electromagnetic and non-electromagnetic part of the hadronic shower is different, with the consequence that the electromagnetic ( $e$ ) to hadronic ( $\pi$ ) signal ratio  $e/\pi \neq 1$ . The performance of hadron calorimeters is then determined by their relative response to the electromagnetic ( $e$ ) and hadronic ( $\pi$ ) shower, measured by the  $e/\pi$  signal ratio.

### 3. The local hardening effect

The equalization of the response of a hadron calorimeter with silicon readout to electromagnetic and hadronic showers can be achieved by suppressing the electromagnetic response of the calorimeter when high- $Z$  (Pb, W, U) absorber plates are used. This suppression mainly occurs via multiple scattering when the silicon detectors are inserted in between thin low- $Z$  plates (G10, polyethylene). The thickness of these low- $Z$  plates must be negligible in radiation length compared with that of the high- $Z$  absorber plates.

A large fraction of the initial electron energy goes into the production of low-energy photons during the shower development. These soft photons interact almost exclusively in the absorber and most of them will transfer their energy partly (Compton effect,  $\propto Z$  of the absorber material) or totally (photoelectric effect  $\propto Z^5$  of the absorber material) to the electrons of the absorber. As a consequence, low-energy photons from the electromagnetic shower development may convert into electrons sufficiently close to the surface of the absorber plate for them to escape and normally to contribute to the measured signal. These low-energy electrons may be multiply-scattered. In high- $Z$  material, the low-energy electrons form larger angles  $\alpha$  with respect to the shower axis than in low- $Z$  material:

$$\langle \cos\alpha \rangle \approx \cos(21 \text{ MeV}/\epsilon\pi),$$

where  $\epsilon$  is the critical energy as given by eq. (2). The number of large-angle electrons (decreasing as  $\epsilon^2$ ) is large in high- $Z$  material and small in low- $Z$  material. Multiple scattering increases the path-length of the electrons: their path-length  $d$  becomes  $d' \equiv d/\langle \cos\alpha \rangle$ . The net effect of multiple scattering is to create a flux of backward-going electrons in the

absorber. These soft electrons can be absorbed by the G10 plates inserted between the active and absorber planes and, therefore, are responsible for the decrease of the visible energy: the local hardening effect [6]. It was observed, for instance, that the response of a Si/U calorimeter can be reduced by 29% in the case where the 5.0 mm G10 absorber is located (only) behind the detectors (see fig. 1).

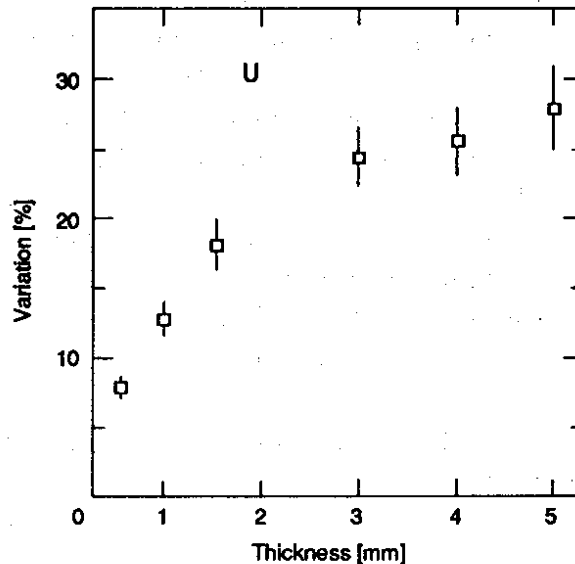


Fig. 1: The variation (in %) of the response of a Si/U calorimeter (see ref. [7]) as a function of the thickness of G10 absorbers located (only) behind side of the detectors.

This suppression leads to a reduction by about 20% of the ratio of the electromagnetic to the non-electromagnetic shower component. The degree of hardening depends on the thickness of the low- $Z$  absorber (small so far in radiation length compared with that of the high- $Z$  material) allowing the fine tuning of the calorimeter response to electromagnetic showers. In a first approximation, the  $e/mip$  ratio for an absorber  $i$  behaves as:

$$e/mip \approx (d'_{Si}/d_{Si})/(d'_i/d_i).$$

Any multiple scattering for a minimum ionizing particle and the energy loss in the active medium of the calorimeter have been neglected. It shows that  $e/mip$  clearly depends on the ratio  $d'/d$  from the multiple scattering. Since  $d'/d > 1$  in a high- $Z$  absorber and  $d'_{Si}/d_{Si} \approx 1$ , one has  $e/mip < 1$ .

#### 4. The filtering effect

For a given absorber  $\sigma_{\text{samp}}$  can easily be modified and eventually decreased by changing the frequency of the sampling (i.e. changing the number of active planes per interaction length ( $\lambda$ ) and/or changing the ratio between the relative thicknesses of the readout and the absorber [7]. The magnitude  $\sigma_{\text{intr}}$  of the fluctuation is sensitive to the number of neutrons released by the absorber per GeV of incident energy [7].  $\sigma_{\text{intr}}$ , being then intrinsic to the absorber material, can be minimized by an adequate choice of the absorber. For instance  $\sigma_{\text{intr}}/E = 45\%/\sqrt{E}$  for a uranium absorber and  $18\%/\sqrt{E}$  for an Fe absorber.

Therefore aiming at an energy resolution of  $\sigma/E = 50\%/\sqrt{E}$  leads to the concept of a calorimeter with a Fe-dominated absorber and a fraction of high- $Z$  metal. This creates a situation where the compensation condition has to be achieved in a silicon calorimeter with a combination of low- $Z$  (Fe) and high- $Z$  (the choice is Pb) as the passive medium. In that case, the thickness of the low- $Z$  material is no longer negligible compared to the thickness of the high- $Z$  material when expressed in radiation lengths. Interspersing low- $Z$  layers in a high- $Z$  material leads to sizeable effects. The combination of Pb and Fe leads to an electromagnetic shower energy transformation effect, generated by a sharp transition from small to large values of the critical energy ( $\epsilon = 7.4$  MeV and 21.0 MeV for Pb and Fe, respectively). Because the value of  $\epsilon$  coincides with that value of the electron energy below which ionization energy loss starts to dominate the energy loss by bremsstrahlung, the increase of the critical energy of the absorber favours the ionization energy loss with respect to the energy loss by radiation. The energy spectra of incident electrons become softer when moving from a high- $Z$  absorber to a low- $Z$  (Fe) absorber. The low- $Z$  (Fe) part of the absorber produces a filtering effect [8] on the electrons. As a result, the energy of the shower is transformed and the response of the calorimeter to the incoming shower is dramatically modified.

The degree of lowering of the critical energy obviously depends on the fraction of Fe and Pb in the absorber [8].

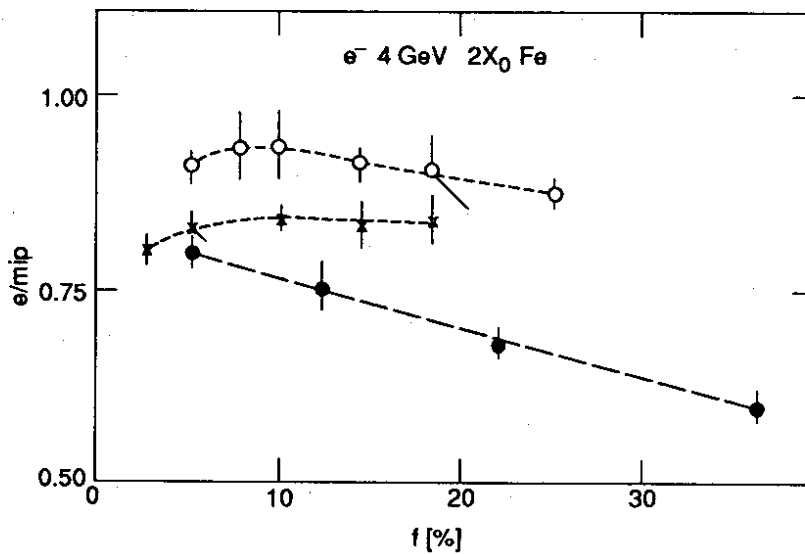


Fig. 2:  $e/mip$  as a function of the Pb fraction  $f$  in the passive absorber [ $f \equiv L_{Pb}/(L_{Pb} + L_{Fe})$ ;  $L_i$  is the thickness of the absorber  $i$ ] for various calorimeter configurations (Fe is  $1.99 X_0$  thick) and for 4 GeV incoming electron energy:  
 (•) PbFe-Si-PbFe, (x) FePb-Si-FePb, and (o) PbFePb-Si-PbFePb.

Figure 2 shows the  $e/mip$  ratio as a function of the Pb fraction,  $f$ , in the passive absorber [ $f \equiv L_{Pb}/(L_{Pb} + L_{Fe})$ ] for various calorimeter configurations ( $L_{Fe} = 1.99 X_0$ ). For the configurations, FePb-Si-FePb and PbFePb-Si-PbFePb, where the forward-generated electrons in Pb can enter the silicon detectors directly, there is an increase of the value of the  $e/mip$  ratio up to  $f \approx (5 - 8)\%$ . For the PbFe-Si-PbFe configuration, where the forward-generated electrons in Pb now enter the Fe absorber,  $e/mip$  is steadily decreasing

and equal to  $0.60 \pm 0.02$  at  $f = 0.36$ .

To summarize, the filtering effect is obtained when combinations of low- $Z$  and high- $Z$  materials are used as absorbers. The action of Fe on Pb, by modifying the critical energy during the electromagnetic shower development, has a net effect in decreasing the number of electrons (the probability of energy losses by collisions is increased) for the forward-going electrons. The effect depends both on the Pb fraction ( $f$ ) (since the fraction of low-energy electrons is proportional to  $f$ ) and on the Fe sampling thickness (because this thickness defines the maximum absorbable electron energy).

## 5. Compensating calorimetry

### 5.1 Absorber made of a combination of Fe and Pb

The ability to modify  $(e/mip)_{\text{Fe+Pb}}$  implies the possibility of tuning the  $e/\pi$  ratio with the fraction of Pb in the absorber. Using eqs. (5) and (6a), the visible energy can be written as

$$\epsilon_{\text{vis}}(\pi) = (e/\pi) \left[ \frac{(h/mip)E_s(1 - f_{\text{em}})}{1 - (e/\pi)f_{\text{em}}} \right], \quad (7)$$

and in the case of an absorber composed of Fe and Pb,  $h/mip$  is given by

$$(1/L)[(L_{\text{Pb}}/\lambda_{\text{Pb}})(h/mip)_{\text{Pb}} + (L_{\text{Fe}}/\lambda_{\text{Fe}})(h/mip)_{\text{Fe}}], \quad (8)$$

with  $L \equiv L_{\text{Pb}}/\lambda_{\text{Pb}} + L_{\text{Fe}}/\lambda_{\text{Fe}}$ .

The estimates of  $h/mip$  from Monte Carlo predictions [9] allow a comparison of  $\epsilon_{\text{vis}}$  obtained from  $(h/mip)E_s$  [eq. (7) when the compensation condition  $e/\pi = 1$  is achieved] with  $\epsilon_{\text{vis}}$  measured for the PbFe-Si-PbFe configuration. The comparison provides the exact proportions of Pb and Fe that are necessary to achieve the compensation condition [1,9].

An experimental programme will start at the CERN-SPS in 1991 in order to demonstrate the possibility of obtaining the compensation in a full-size Si/Fe + Pb hadron calorimeter.

### 5.2 Absorber made of uranium

Evidence for the achievement of the compensation condition has been found with a Si/U hadron calorimeter by using the local hardening effect [10]. For instance, the effect of 5 mm thick G10 plates, inserted in front of and behind the Si readout mosaics, is to reduce the electromagnetic visible energy by about 40% while the hadronic visible energy is reduced by about 12% only. This different behaviour for electrons and protons is the essence of the realization of the compensation condition in Si/U hadronic calorimetry. At these incoming proton energies, the average fraction  $f_{\text{em}}$  of the converted electromagnetic energy in a hadronic shower is about 25–30%. The part of the visible energy that is due to the electromagnetic component of the shower is expected to be reduced by the local hardening effect when low- $Z$  (G10) plates are inserted. However, the reinteractions of the hadronic particles in these plates increases the ionizing hadronic component of the shower, since the  $A$ -value of G10 is lower than that of uranium. Thus, when the sampling fraction (defined as the absorber material thickness in units of interaction lengths in between two active planes) is increased by the additional G10 plates, the expected decrease (about 5.7% with 5 mm thick G10 plates in front of and behind the Si mosaics) of the part of the visible energy part that is due to the pure hadronic component of the shower is largely attenuated. Consequently, the addition of low- $Z$  G10 plates allows the tuning of the  $e/\pi$



ratio, mainly by attenuating the calorimeter response to the electromagnetic component of the hadronic shower.

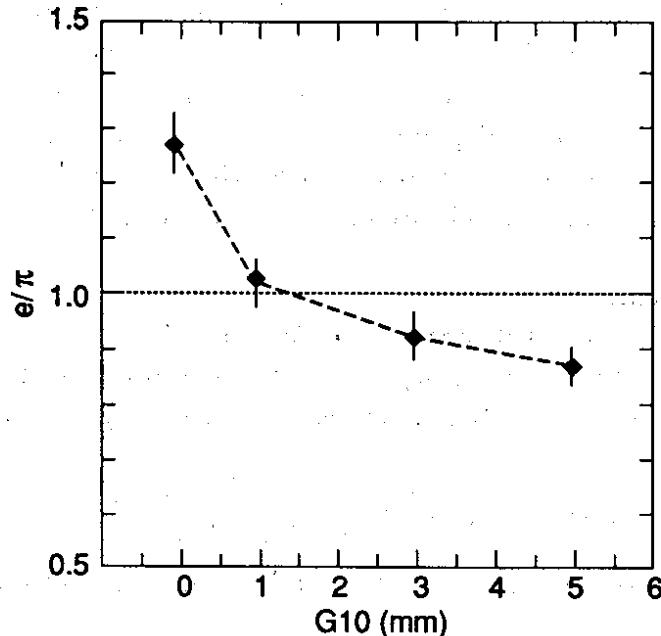


Fig. 3: Measured values of the  $e/\pi$  ratio (see text) as a function of the thickness of additional G10 plates. The line is to guide the eye.

In figure 3, the  $e/\pi$  values (from an average of measurements at incoming particle energies of 8, 10, and 12 GeV [10]) are shown as a function of the thickness of the G10 plates. The thickness of the low- $Z$  G10 plates to be located in front and behind the Si mosaics in order to achieve the compensation condition ( $e/\pi = 1$ ), is estimated [10] to be  $t_g = (1.2 \pm 0.2)$  mm. The local hardening effect has allowed the value of the  $e/\pi$  ratio to be modified by about 34%, when changing to a calorimeter configuration where 5 mm thick G10 plates are inserted both in front of and behind of the silicon detectors.

## 6. Discussion and conclusions

The results of the SICAPO Collaboration demonstrate the effectiveness of the local hardening effect in modifying the response to the incoming showers of a hadronic calorimeter, with silicon readout and a combination of low- $Z$  and high- $Z$  materials as absorbers. This local hardening effect increases the reduction of the visible energy beyond the reduction normally expected from energy sharing. In the case of the Si/U used in the measurements [11], a ratio  $e/\pi = 1$  is obtained resulting from the insertion of G10 plates ( $1.2 \pm 0.2$ ) mm thick in front of and behind the silicon detectors.

The use of a combination of Fe (low- $Z$ ) and Pb (high- $Z$ ) materials as absorbers allows the transformation of the electron energy distribution of the incident showers ('the filtering effect'). The action of the low- $Z$  on the high- $Z$  material, by modifying the critical energy during the electromagnetic shower development, leads to a yield of soft electrons (and very few photons).

The flux of backward-going electrons (resulting from multiple scattering in the high- $Z$  absorber) are absorbed by the thin (in radiation length) G10 plates inserted in the calorimeter configuration between the rear of the active and the passive media ('the local hardening effect').

The local hardening effect has also been measured for polyethylene layers inserted

in front of and behind the silicon mosaics. The level of reduction of the electromagnetic visible energy  $\Delta\epsilon_{\text{vis}}/\epsilon_{\text{vis}}$  is similar to that obtained for G10 [1]. Therefore, polyethylene can be used instead of G10 to achieve the compensation condition ( $e/\pi = 1$ ). The possible use of polyethylene presents the advantage that it can play the role of a neutron moderator as indicated by recent activation studies [11], and may then contribute to reinforcing the radiation hardness of the calorimeter.

All these facts support the choice, for the next generation of colliders, of a hadron calorimeter with silicon as the active medium and a combination of Fe and Pb as absorbers. Silicon indeed allows compact and flexible construction, fine granularity, fast charge collection, and easy calibration. The choice of an absorber made of a combination of Fe and Pb permits the achievement of the compensation condition also through the combined effect of hardening and filtering resulting from the insertion of G10 planes between the readout and the absorber which consists of a mixture of low- $Z$  and high- $Z$  metals [8]. As a consequence, a linear response of the calorimeter to hadronic showers and a good energy resolution, improving as the incident energy increases, can be obtained. In addition, an increase of the radiation hardness is possible with the insertion of polyethylene foils, which have basically the same properties as G10, and increase the pure hadronic response (i.e.  $h/\text{mip}$  value).

## REFERENCES

- [1] E. Borchi et al. (SICAPO Collaboration), Silicon sampling hadronic calorimetry: a tool for experiments at the next generation of colliders, presented by C. Leroy at the Int. Conf. on Advanced Technology and Particle Physics, Como, 1988 [Nucl. Instrum. Methods **A279** (1989)], p. 57;  
C. Bertrand et al. (SICAPO Collaboration), Silicon calorimetry for the SSC, Summary report of the silicon calorimetry working group, OREXP-89-0902, Proc. of the Workshop on Calorimetry for the Superconducting Super Collider, The University of Alabama, Tuscaloosa, Alabama, USA, 1989, eds. R. Donaldson and M.G.D. Gilchriese (World Scientific, Singapore, 1990), p. 489.
- [2] Y.S. Tsai, Rev. Mod. Phys. **46** (1974) 815.
- [3] U. Amaldi, Physica Scripta **23** (1981) 409.
- [4] O.I. Dovzhenko and A.A. Pomanskii, Sov. Phys. JETP **18** (1964) 187.
- [5] C.W. Fabjan, Calorimetry in high energy physics, CERN-EP/85-54 (1985).
- [6] F. Lemeilleur et al. (SICAPO Collaboration), Phys. Lett. **B222** (1989) 518.
- [7] C. Leroy, Y. Sirois and R. Wigmans, Nucl. Instrum. Methods **A252** (1986) 4; R. Wigmans, Nucl. Instrum. Methods **A259** (1987) 389.
- [8] E. Borchi et al. (SICAPO Collaboration), Phys. Lett. **B222** (1989) 526.
- [9] J.E. Brau and T.A. Gabriel, Theoretical studies of hadronic calorimeters for high-luminosity, high-energy colliders, presented by J.E. Brau at the Int. Conf. on Advanced Technology and Particle Physics, Como, 1988 [Nucl. Instrum. Methods **A279** (1989)], p. 40.
- [10] A.L.S. Angelis et al. (SICAPO Collaboration), Phys. Lett. **B242** (1990) 293.

- [11] E. Borchini et al. (SICAPO Collaboration), presented by R. Steni at the ECFA Study Week on Instrumentation Technology for High-Luminosity Hadron Colliders, Barcelona, Spain, 1989.